The Conserved KMN Network Constitutes the Core Microtubule-Binding Site of the Kinetochore

Iain M. Cheeseman,[1,*] Joshua S. Chappie,[2] Elizabeth M. Wilson-Kubalek,[2] and Arshad Desai[1,*]
[1] Ludwig Institute for Cancer Research, Department of Cellular and Molecular Medicine (UCSD), CMM-East, Room 3052, La Jolla, CA 92093, USA
[2] Center for Integrative Molecular Biosciences, Department of Cell Biology, The Scripps Research Institute, 10550 North Torrey Pines Road, La Jolla, CA 92037, USA
*Contact: icheeseman@ucsd.edu (I.M.C.), abdesai@ucsd.edu (A.D.)

SUMMARY

The microtubule-binding interface of the kineto-chore is of central importance in chromosome segregation. Although kinetochore compo-nents that stabilize, translocate on, and affect the polymerization state of microtubules have been identified, none have proven essential for kinetochore-microtubule interactions. Here, we examined the conserved KNL-1/Mis12 com-plex/Ndc80 complex (KMN) network, which is essential for kinetochore-microtubule interac-tions in vivo. We identified two distinct microtu-bule-binding activities within the KMN network: one associated with the Ndc80/Nuf2 subunits of the Ndc80 complex, and a second in KNL-1. For-mation of the complete KMN network, which additionally requires the Mis12 complex and the Spc24/Spc25 subunits of the Ndc80 com-plex, synergistically enhances microtubule-binding activity. Phosphorylation by Aurora B, which corrects improper kinetochore-microtu-bule connections in vivo, reduces the affinity of the Ndc80 complex for microtubules in vitro. Based on these findings, we propose that the conserved KMN network constitutes the core microtubule-binding site of the kinetochore.

INTRODUCTION

In the late nineteenth century, a differentiated chromo-somal region that connects to spindle fibers during mitosis was first described (reviewed in Schrader, 1953). Electron microscopy provided a direct view of this region, termed the kinetochore, and demonstrated that microtubule plus ends directly embed in the outer kinetochore plate (reviewed in Rieder, 1982). However, these are not static attachments, and chromosome movement is intimately coupled to changes in the polymerization dynamics of kinetochore-bound microtubules (Maddox et al., 2003; Rieder and Salmon, 1998). More recently, the identifica-tion of numerous kinetochore proteins and elucidation of their in vivo loss-of-function phenotypes is providing a molecular view of this structure. Despite this progress, the identity of the core microtubule-binding site of the ki-netochore has remained elusive. Most significantly, com-ponents that both are essential in vivo for kinetochore-microtubule interactions and exhibit direct interactions with microtubules in vitro have not been identified.

A variety of approaches in different organisms have identified kinetochore components that interact with mi-crotubules (reviewed in Cleveland et al., 2003; Maiato et al., 2004). These include the Dam1 ring complex, the plus end-tracking proteins CLASP, CLIP-170, and EB1, the minus end-directed microtubule motor dynein, the plus end-directed kinesin-7 (CENP-E), and the microtubule de-polymerizing kinesin-13 (Kin I) and kinesin-8 (Kip3). How-ever, while these proteins make important contributions to chromosome movement, in vivo inhibitions indicate that none of them are essential for the stable interaction of kinetochores with microtubules. Recently, the Dam1 ring complex in budding yeast has received attention as a potential kinetochore-spindle connector. Although mu-tational inactivation of the Dam1 complex causes severe chromosome missegregation, it does not eliminate all ki-netochore-spindle interactions (Cheeseman et al., 2001). In addition, this complex is genetically dispensable for via-bility in fission yeast (Sanchez-Perez et al., 2005) and is not detectably conserved outside fungi. In metazoans, inhibi-tion of the two kinetochore motors (cytoplasmic dynein and CENP-E) does not significantly alter chromosome-spindle interactions for the majority of chromosomes (Ho-well et al., 2001; Putkey et al., 2002). Inhibition of CLASP family proteins specifically inhibits microtubule polymeri-zation at kinetochores (Maiato et al., 2005) but does not prevent the formation of kinetochore-microtubule attach-ments. In total, the analysis of currently identified microtu-bule-binding proteins fails to account for the activity of the core microtubule-binding site of the kinetochore.

We previously used a combination of biochemistry and functional genomics in *C. elegans* to identify a network of 10 interacting proteins that plays a central role at the kinetochore-microtubule interface (Cheeseman et al., 2004; Desai et al., 2003). Phenotypic analysis by single-cell assays partitioned the components of this network into three distinct groups (see Figure 1A). Depletion of the "KNL" proteins KNL-1 (termed Spc105 in budding yeast; Nekrasov et al., 2003) or KNL-3 completely abolished kinetochore-microtubule interactions. Depletion of the second group, equivalent to the Mis12 complex in other organisms (De Wulf et al., 2003; Kline et al., 2006; Obuse et al., 2004), compromised kinetochore assembly. Depletion of the third group, equivalent to the Ndc80 complex (DeLuca et al., 2005; McCleland et al., 2004; Wigge and Kilmartin, 2001), resulted in kinetochores that were unable to sustain tension during interactions with spindle microtubules. Most importantly, the KNL-1/Mis12 complex/Ndc80 complex (KMN) network is conserved throughout eukaryotes and is essential for viability and kinetochore-microtubule interactions in multiple organisms (reviewed in Kline-Smith et al., 2005). However, whether the KMN network plays a direct or indirect role in kinetochore-microtubule interactions remains unresolved. The importance of this network in outer kinetochore assembly has led to the general hypothesis that it makes an indirect structural contribution (see Joglekar et al., 2006).

Here we investigate the organization and activity of the KMN network using purified components in vitro. We identify two distinct microtubule-binding activities within the network—one intrinsic to the Ndc80 and Nuf2 subunits of the Ndc80 complex, and a second intrinsic to KNL-1. Reconstitution of the entire network by combining its component parts strongly enhances the net microtubule-binding affinity. We further define the molecular connectivity of the KMN network and provide evidence that the microtubule-binding activity of the Ndc80 complex is regulated by Aurora B kinase phosphorylation of the Ndc80 subunit. Based on these findings, and in light of previous in vivo studies, we propose that the conserved KMN network constitutes the core microtubule-binding site of the kinetochore.

RESULTS

Partially Purified *C. elegans* KMN Protein Network Cosediments with Microtubules
We previously isolated a conserved network of interacting kinetochore proteins from *C. elegans* consisting of KNL-1, KNL-3, phenotypically defined groups of NDC proteins (NDC-80, Nuf2[HIM-10], Spc25[KBP-3]), and MIS proteins (MIS-12, KBP-1, KBP-2), which we proposed were equivalent to the yeast and human Ndc80 and Mis12 kinetochore subcomplexes, respectively, and a nonessential protein KBP-5 (Cheeseman et al., 2004). Consistent with the severity of their depletion phenotypes, KNL-3 is required to recruit KNL-1, which is in turn required to recruit the NDC-80 subcomplex (summarized in Figure 1A;

Cheeseman et al., 2004). Here, we will refer to this group of interacting proteins as the KMN network for KNL-1, Mis12 complex, and Ndc80 complex.

To determine whether the KMN network has a direct or indirect role in forming kinetochore-microtubule attachments, we used the first steps of a tandem affinity purification scheme to enrich the endogenous KMN network (Cheeseman et al., 2004). The partially purified network cosedimented with taxol-stabilized microtubules (Figure 1B). No pelleting was observed in the absence of microtubules, and all tested network subunits cosedimented equivalently (Figure 1B; not shown). Varying the microtubule concentration and quantifying the percent copelleted KMN network indicated that, assuming ∼60% of the input material is competent for binding, half-maximal binding occurs at ∼0.75 μM (Figure 1C). We conclude that the KMN network is closely associated with a direct microtubule-binding activity with an apparent dissociation constant (K_{Dapp}) in the submicromolar range.

Reconstitution of the KMN Network via Bacterial Coexpression
Partially purified KMN network sedimented with microtubules, but we could not exclude the possibility that a copurifying protein accounts for this microtubule-binding activity. Therefore, we reconstituted the network by utilizing a bacterial polycistronic expression system that facilitates coexpression of multiple open reading frames (Tan, 2001). The reconstitution was guided by previous in vivo analysis (Cheeseman et al., 2004; Desai et al., 2003), along with work in other organisms that suggested that groups of proteins within the network are likely to form discrete subcomplexes. We did not express KBP-5, which is dispensable for viability in *C. elegans*.

NDC-80 Complex
A 4-subunit Ndc80 complex (Ndc80, Nuf2, Spc24, and Spc25) exists in fungi and vertebrates (McCleland et al., 2004; Wigge and Kilmartin, 2001). Sequence homology and our previous in vivo experiments identified three likely NDC-80 complex subunits in *C. elegans*: NDC-80, Nuf2[HIM-10], and Spc25[KBP-3] (Cheeseman et al., 2004). Weak sequence similarity and in vivo analysis led us to suspect that KBP-4 is equivalent to Spc24 in other organisms. Consistent with this, KBP-4 copurified with the other subunits through multiple purification steps resulting in a nearly homogenous 4-subunit NDC-80 complex (Figure 1D).

KNL-3 and the MIS Proteins
Attempts to express KNL-3 on its own were unsuccessful (Figure 1E). Since in vivo analysis indicated that the MIS proteins (MIS-12, KBP-1, and KBP-2) make an important contribution to kinetochore assembly by affecting KNL-3 recruitment (Figure 1A; Cheeseman et al., 2004), we tested whether coexpression with the MIS proteins facilitated KNL-3 expression. Coexpression of KBP-1, but not the unrelated protein GST, resulted in detectable KNL-3 expression (Figure 1E). This stabilization of expression was enhanced when the complete set of MIS proteins

was present. We observed a strikingly similar stabilization effect for the hDsn1 subunit of the human Mis12 complex during bacterial coexpression (data not shown; Kline et al., 2006), which leads us to suggest that KNL-3 is the *C. elegans* counterpart of hDsn1. Consistent with this, KBP-1, KBP-2, and MIS-12 copurified with KNL-3-6xHis from bacteria through multiple purification steps (Figure 1F; see Figure S1 in the Supplemental Data available online), although excess KNL-3 is present in the final purified material relative to the other subunits. KNL-3 is the functionally critical component of this complex, because its depletion abolishes kinetochore-microtubule interactions in vivo. However, for consistency with work in other organisms, we will refer to this group of four interacting proteins as the MIS-12 complex.

KNL-1 and KNL-1/MIS-12 Complex

We were also able to purify full-length KNL-1-6xHis on its own (Figure 1G). However, the large size of KNL-1 prevented robust expression and resulted in some smaller molecular weight products because of either degradation or the use of alternative start codons during translation. If KNL-1-6xHis and untagged KNL-3/MIS-12/KBP-1/KBP-2 were expressed together, all of the expressed proteins copurified (Figure 1H; Figure S1), although the stoichiometry of MIS-12 was lower in the final gel filtration step when compared to the MIS-12 complex purified with tagged KNL-3 (Figure 1F; Figure S1). This result indicates that KNL-1 directly interacts with the MIS-12 complex. We will refer to the material obtained by this copurification as KNL-1/MIS-12 complex.

Reconstitution of the KMN Network from Its Constituent Parts

To determine whether the KMN network can be reconstituted from KNL-1, the MIS-12 complex, and the NDC-80 complex in the absence of additional proteins, we performed gel filtration chromatography. Individually, the NDC-80 and MIS-12 complexes have stokes radii of ~85 Å and 48 Å, respectively (Figure 2A, gels 1 and 3), consistent with work on their counterparts in humans and budding yeast (Ciferri et al., 2005; De Wulf et al., 2003; Kline et al., 2006; Wei et al., 2005). KNL-1 fractionated near the void volume of the column, suggesting that it is oligomeric (Figure 2A, gel 2). Sucrose gradient sedimentation indicated an S value of ~16 (not shown), supporting the existence of an oligomer of 5–10 KNL-1 molecules. Importantly, this fractionation profile of recombinant KNL-1 is similar to that of endogenous KNL-1 in the presence of both low (50 mM) and high (750 mM) salt (Figure S2).

We next conducted gel filtration of equimolar mixtures to test whether the network can be reconstituted with the individual components and to define the network connectivity. For the KNL-1/MIS-12 complex mixture purified with a single tag on KNL-1 (Figure 1H), a significant pool of the MIS-12 complex cofractionated with KNL-1 (Figure 2A, gel 4), confirming the existence of a direct interaction. Mixing the NDC-80 complex with either KNL-1 (N + K) or the MIS-12 complex (N + M) did not shift the migration

of either component, suggesting that they do not interact directly (Figure 2A, gels 5 and 6). However, when the NDC-80 complex was combined with KNL-1/MIS-12 complex, a significant pool of the NDC-80 complex shifted to a higher molecular weight range (Figure 2A, gel 7), resulting in an overall fractionation profile similar to that of the endogenous KMN network (Figure S2).

Densitometry of Coomassie-stained gel filtration fractions indicated stoichiometric amounts of NDC-80, Nuf2[HIM-10], and KNL-3 (Figure 2B; data not shown). KBP-1, KBP-2, Spc24[KBP-4], and Spc25[KBP-3] were also stoichiometric relative to each other in peak fractions. For KNL-1, where a series of lower molecular weight species are present, stoichiometry measurements were not possible. MIS-12 was present at a lower stoichiometry relative to the other proteins but was clearly present in the peak fractions (also see Figure S1). In total, these results define the connectivity of the KMN network and indicate that this network can be reconstituted from the components identified in our previous study in the absence of other eukaryotic proteins.

Two Distinct Microtubule-Binding and -Bundling Activities Are Present in the KMN Network

Previous studies in multiple organisms have demonstrated that the Ndc80 complex is essential for robust kinetochore-microtubule interactions (reviewed in Kline-Smith et al., 2005). However, it remained unclear whether the Ndc80 complex binds directly to microtubules or forms an indirect connection through a binding partner. To address this question, we examined the ability of the NDC-80 complex to cosediment with GMPCPP (Figure 3A) or taxol-stabilized microtubules (not shown). The NDC-80 complex did not pellet on its own or in the presence of monomeric GDP-tubulin (Figure 3A; not shown), but it cosedimented with both stabilized microtubule substrates. Mixing limiting amounts of the NDC-80 complex (50 nM) with varying concentrations of microtubules revealed a weak apparent binding affinity ($K_{Dapp} > 3 \mu M$). At a 20-fold higher concentration of NDC-80 complex (1 μM; Figure 3A), more robust cosedimentation was observed. Further analysis revealed an anomalous behavior that precluded fitting the data points to a simple binding isotherm and suggested a more complex cooperative mechanism (see below and Figure S3). We conclude that the widely conserved Ndc80 complex, which is critical for kinetochore-spindle interactions in vivo, binds directly to microtubules in vitro, albeit with low affinity when present at limiting concentrations.

Similar experiments with purified KNL-1 revealed a second microtubule-binding activity in the KMN network (Figure 3B). At ~50 nM KNL-1, only minor cosedimentation was detected, even at high microtubule concentrations. However, increasing the concentration of KNL-1 3-fold dramatically increased the amount of cosedimenting protein (Figure 3B). No cosedimentation with microtubules was detected for the MIS-12 complex alone (Figure 3B). However, when KNL-1/MIS-12 complex was
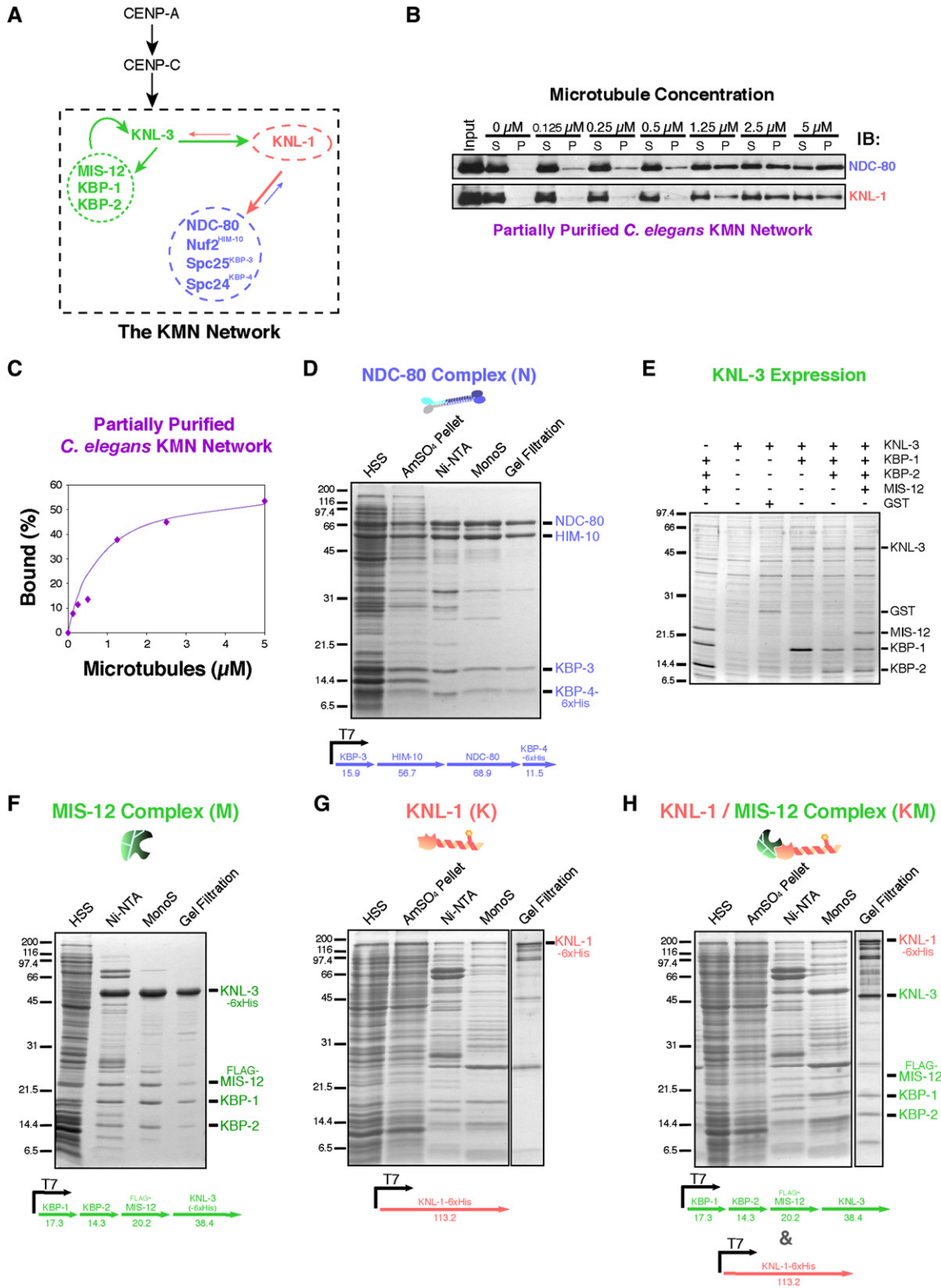
Figure 1. Microtubule Binding of the Endogenous KMN Network and Reconstitution of Network Components in Bacteria

(A) Schematic of the *C. elegans* KMN network depicting in vivo kinetochore localization dependencies. Dashed circles indicate phenotypically clustered groups of MIS (green) and NDC (blue) proteins.

used as the input, the MIS-12 complex cosedimented with microtubules in a manner mimicking KNL-1 (Figure 3B). The percent of input complex competent to bind microtubules and the apparent affinity of the KNL-1/MIS-12 complex were higher than for KNL-1 alone, which may reflect stabilization of KNL-1 by coexpression with MIS-12 complex.

In addition to binding directly to microtubules, the NDC-80 complex, KNL-1, and the KNL-1/MIS-12 complex bundled microtubules in vitro (Figure 3C; data not shown). With 1 μM microtubules, approximately 2-fold molar excess of NDC-80 was required to observe robust bundling, whereas only a ∼1:4 molar ratio of KNL-1/MIS-12 complex was necessary, possibly reflecting the oligomeric state of KNL-1. The bundling observed with both components may contribute to the concentration dependence observed in the cosedimentation analysis. Cumulatively, these results indicate that there are two independent microtubule-binding and -bundling activities in the KMN network: one in the NDC-80 complex and a second in KNL-1.

Reconstitution of the KMN Network Results in a Synergy between the Microtubule-Binding Activities of the NDC-80 Complex and KNL-1

Above, we demonstrated that KNL-1 and the NDC-80 complex bind to microtubules and that the KNL-1/MIS-12 complex interacts with the NDC-80 complex. We next tested the microtubule-binding activity of mixtures of the three parts of the network. For these experiments, we used limiting amounts of each component (50 nM) to maximize the sensitivity for detecting changes in the apparent microtubule-binding affinity. Consistent with the lack of an observed interaction between the NDC-80 complex and, individually, KNL-1 or the MIS-12 complex (Figure 2A), the corresponding mixtures did not exhibit changes in the microtubule-binding activity of the input components (Figure 4A; compare with Figures 3A and 3B, 50 nM panels). In contrast, mixing the KNL-1/MIS-12 complex and the NDC-80 complex, which reconstitutes the KMN network (Figure 2A), resulted in a dramatically increased apparent microtubule-binding affinity relative to

the individual components (Figures 4B and 4C). Half-maximal binding occurred at ∼0.5 μM microtubules, which indicates that the apparent binding affinity at this input concentration is similar to what is observed with the partially purified endogenous KMN network (Figures 1B and 1C). Thus, the connection between the NDC-80 complex and KNL-1 within the KMN network synergizes their individual microtubule-binding activities.

The KNL-1/MIS-12 Complex and the NDC-80 Complex Exhibit Cooperative Binding to Microtubules

KNL-1, the KNL-1/MIS-12 complex, and the NDC-80 complex exhibit significant differences in microtubule binding when their input concentration is varied. To explore this behavior further, we fixed the microtubule concentration at 5 μM and varied the KMN network components between 50 nM and 500 nM. Under these conditions, microtubules are in significant excess, and the percent cosedimented complex should remain relatively constant for a simple binding interaction. The NDC-80 complex largely followed this expectation (Figures 4D and 4E). In contrast, KNL-1/MIS-12 complex exhibited steep concentration dependence, with the amount of cosedimented complex increasing from 10% to 90% (Figures 4D and 4E). The reconstituted KMN network followed a similar but less dramatic trend, although this conclusion is limited by the significant binding present at even the lowest tested concentration (Figures 4D and 4E). We suspect that this apparent cooperative binding reflects the oligomeric nature of KNL-1 and its potent bundling activity.

For the NDC-80 complex, where testing a higher concentration range (1–5 μM) was feasible, the amount of cosedimented NDC-80 complex exceeded that expected from the estimated weak affinity at lower input concentrations (Figures 4D and 4E; Figure S3). This finding suggests potential cooperativity of NDC-80 complex binding at high fractional occupancy on the microtubule lattice and may also be related to the bundling observed at these concentrations. Scatchard plots confirmed the anomalous binding of both KNL-1/MIS-12 complex and the NDC-80

(B) Microtubule cosedimentation analysis of the endogenous KMN network partially purified from a *C. elegans* strain stably expressing LAP-tagged (GFP-TEV-S peptide) KBP-1 (Cheeseman et al., 2004). The material eluted by TEV cleavage was used for cosedimentation with the indicated concentrations of taxol-stabilized microtubules and analyzed by western blotting of supernatant (S) and pellet (P) fractions for KNL-1 and NDC-80. Other network subunits (KNL-3, KBP-1, KBP-2, KBP-3, and KBP-4) showed similar behavior (not shown).

(C) Graph quantifying the microtubule cosedimentation of the endogenous KMN network via the NDC-80 and KNL-1 western blot signals from (B). The line is a theoretical curve for a bimolecular interaction with a 0.75 μM dissociation constant (K_D), 60% of the input material competent to bind, and limiting (<50 nM) concentration of the partially purified network.

(D) Expression and purification of the NDC-80 complex. Top, Coomassie-stained gel of the purification. Bottom, schematic of the construct used to coexpress the four subunits. Predicted molecular weights for each protein are indicated.

(E) KNL-3 expression requires coexpression with the MIS proteins. Coomassie-stained gel showing *E. coli* lysates expressing the indicated proteins. In each case, a single polycistronic plasmid was used. KNL-3 is not detectable when expressed on its own, or when coexpressed with GST, but is detectable when coexpressed with the MIS proteins.

(F) Purification of the MIS-12 complex. Top, Coomassie-stained gel of the purification. Bottom, schematic of the construct used to coexpress the three MIS proteins and KNL-3.

(G) Purification of KNL-1. The left portion of the gel documenting the purification is Coomassie stained; the final lane is silver stained. Bottom, diagram of the KNL-1-6xHis expression construct.

(H) Purification of KNL-1/MIS-12 complex with a single 6xHis tag on KNL-1 as in (G). See also Figure S1. Schematics representing the different components of the KMN network are shown in (D)–(H). These schematics will be used in all subsequent figures.
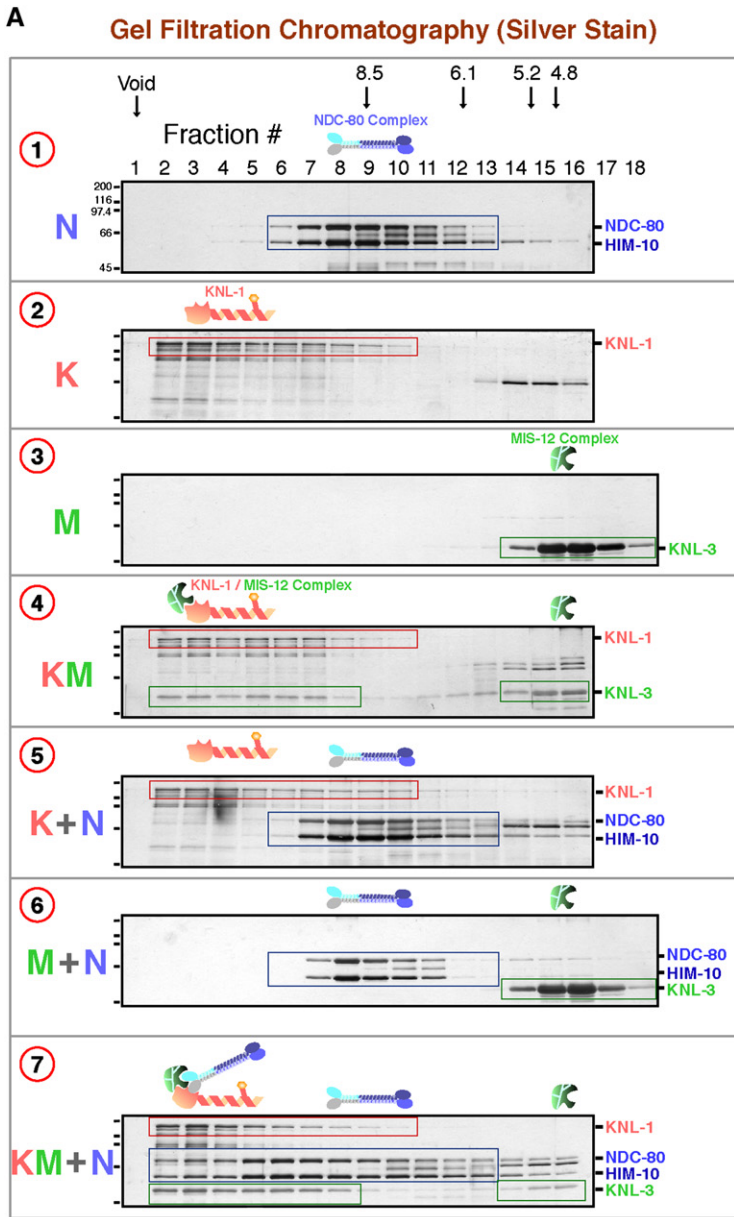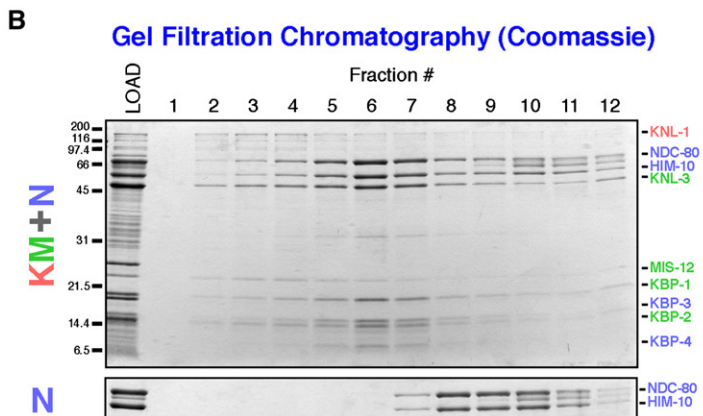
Figure 2. Reconstitution of the KMN Network from Its Expressed Component Parts

(A) Silver-stained gels showing the gel filtration elution profiles of purified NDC-80 complex (N), KNL-1 (K), MIS-12 complex (M), copurified KNL-1/MIS-12 complex (KM), and the indicated mixtures. All input complexes were adjusted to ~1 μM concentration in the column load. Only the gel region where the migration of KNL-1, NDC-80, HIM-10, and KNL-3 is visible is shown. Schematics above each gel panel and colored boxes on the gel images indicate the elution positions of the components and the predicted nature of these complexes. Stokes radii of standards: Thyroglobulin (8.5 nm), Ferritin (6.1 nm), Catalase (5.2 nm), Aldolase (4.8 nm).

(B) Top, Coomassie-stained gel showing the elution profile of the mixture of the NDC-80 and KNL-1/MIS-12 complexes. Bottom, portion of Coomassie-stained gel showing the elution of the NDC-80 complex alone.
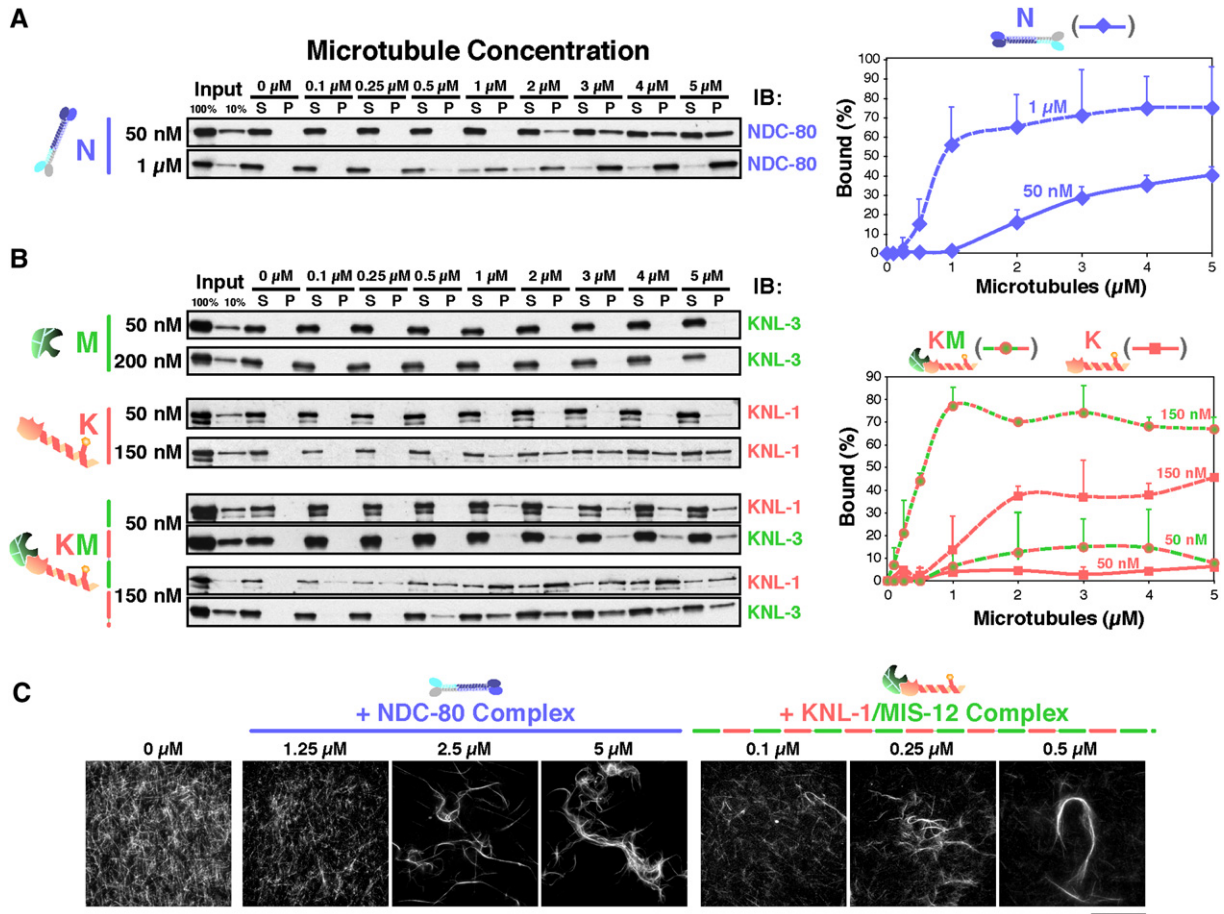
Figure 3. Two Distinct Microtubule-Binding Activities Are Present within the KMN Network

(A) Cosedimentation of purified NDC-80 complex at the indicated microtubule concentrations. The percentage of 50 nM (n = 9) and 1 μM (n = 2) input complex in the supernatant (S) and pellet (P) fractions was monitored by NDC-80 immunoblotting. Right, the average percent bound complex is plotted relative to microtubule concentration. Error bars represent standard deviation.

(B) Cosedimentation of the MIS-12 complex (M; detected by probing for KNL-3), KNL-1 (K; detected by probing for KNL-1), and KNL-1/MIS-12 complex (KM; detected by probing for KNL-1 and KNL-3) at the indicated microtubule concentrations. Two different input concentrations were tested for each component as indicated. The average percent bound KNL-1 and KNL-1/MIS-12 complex, monitored by KNL-1 immunoblotting from two independent experiments, is plotted relative to microtubule concentration on the right. Error bars represent standard deviation.

(C) The NDC-80 and KNL-1/MIS-12 complexes bundle microtubules. 1 μM CY3-labeled GMPCPP microtubules were imaged either alone (left), in the presence of 1.25–5 μM NDC-80 complex, or in the presence of 0.1–0.5 μM KNL-1/MIS-12 complex. Bundling was also observed with KNL-1 alone (not shown). Scale bar represents 40 μm.

complex (Figure S3) and highlighted their distinction from the well-characterized microtubule-binding protein tau, which shows a reduction in apparent binding affinity with increasing concentration (Kar et al., 2003). The concentration dependence of the binding observed for the KMN network components may reflect features important in the in vivo context where a high-density array of this network is organized at the outer kinetochore plate.

Ultrastructural Analysis of NDC-80 Complexes Bound to Microtubules

To directly visualize binding of the NDC-80 complex to microtubules, we performed negative stain electron microscopy. These experiments utilized saturating amounts of the NDC-80 complex, which we estimate results in approximately 1–2 complexes bound per tubulin heterodimer (Figure 5A). After negative staining, we observed the presence of rod-shaped NDC-80 complexes bound along the lengths of the microtubule lattices. The rod shape is consistent with work on the architecture of this complex in the absence of microtubules (Ciferri et al., 2005; Wei et al., 2005). Strikingly, the NDC-80 complex rods bound at an angle relative to the lattice, resembling the barbs generated on actin filaments by myosin decoration (Figure 5B). Binding along a single microtubule polymer occurred with a consistent polarity. In addition, we observed interactions between complexes on neighboring microtubules resulting in crossbridges and bundles.
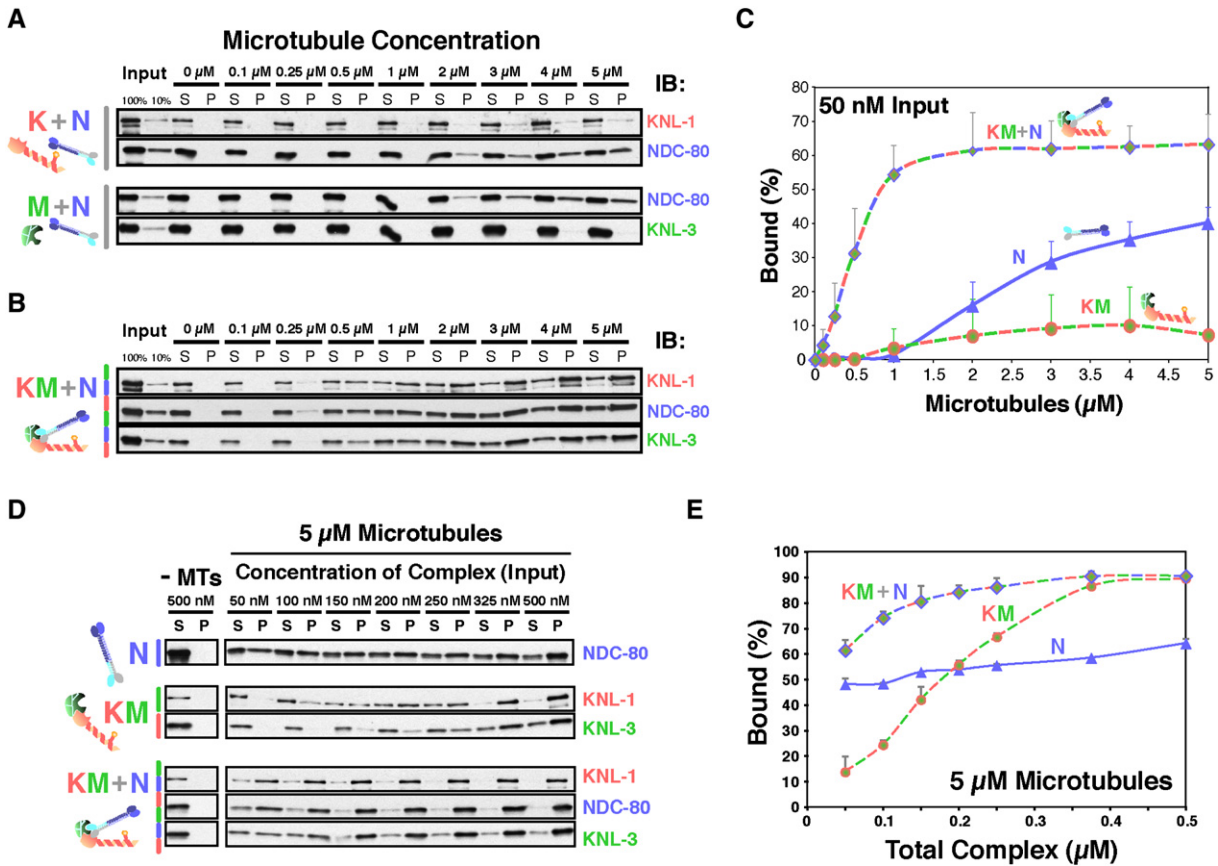
Figure 4. Synergy in Microtubule-Binding Activity after Interaction of the NDC-80 Complex and KNL-1 in the KMN Network
(A) Cosedimentation analysis of mixtures of the MIS-12 complex and the NDC-80 complex (M+N; monitored by KNL-3 and NDC-80 immunoblotting) or of KNL-1 and the NDC-80 complex (K+N; monitored by KNL-1 and NDC-80 immunoblotting). The final concentration of each network component was 50 nM. No significant difference from the individual component cosedimentation analysis (see Figure 3) was observed.
(B) Cosedimentation analysis of KNL-1/MIS-12 complex plus NDC-80 complex mixture (KM+N; each at ~50 nM), monitored by KNL-1, KNL-3, and NDC-80 immunoblotting. Increased cosedimentation is observed for all three network components.
(C) The averaged signal for all three blotted proteins in the KM+N mixture from four different experiments is plotted versus microtubule concentration. For comparison, data for the NDC-80 complex (N) and KNL-1/MIS-12 complex (KM) is replotted from Figure 3. Error bars represent standard deviation.
(D) Concentration-dependent microtubule binding of the KMN network. The concentration of input complexes (N, KM, and KM+N) was varied over the maximal range possible with the microtubule concentration held constant at 5 μM. Loading of supernatant and pellet fractions was adjusted relative to the lowest tested concentration (50 nM) to allow comparison across the entire tested concentration range.
(E) Graph depicting the average percent bound complex over a 50–500 nM input range from two different experiments. Error bars represent standard deviation.

These results confirm that the NDC-80 complex binds to microtubule polymers directly in vitro, and the low-resolution view of this interaction suggests that the microtubule-binding domain is at or near one end of this rod-shaped complex.

The NDC-80 Complex Head Binds to Microtubules, but Not to KNL-1/MIS-12 Complex
Previous work has demonstrated that the Ndc80 and Nuf2 subunits of the Ndc80 complex form a dimer with their globular N-terminal domains extending out from a rod formed by interaction of their coiled coil domains (Ciferri et al., 2005; Wei et al., 2005). The Ndc80/Nuf2 dimer in turn interacts with a Spc24/Spc25 dimer. To investigate the localization of the two distinct activities of the NDC-80 complex—microtubule binding and interaction with the KNL-1/MIS-12 complex—we isolated untagged NDC-80/Nuf2[HIM-10] dimer by using a similar coexpression and purification strategy to the intact NDC-80 complex and by exploiting an intrinsic affinity for nickel agarose independently of an introduced tag (Figure 6A). We will refer to this as the NDC-80 complex head. The NDC-80 complex head bound directly to microtubules in vitro (Figures 6C and 6D) and also strongly bundled microtubules (Figure 6F). Negative stain EM of head-saturated microtubules revealed fine rod-like elements along the lattice with
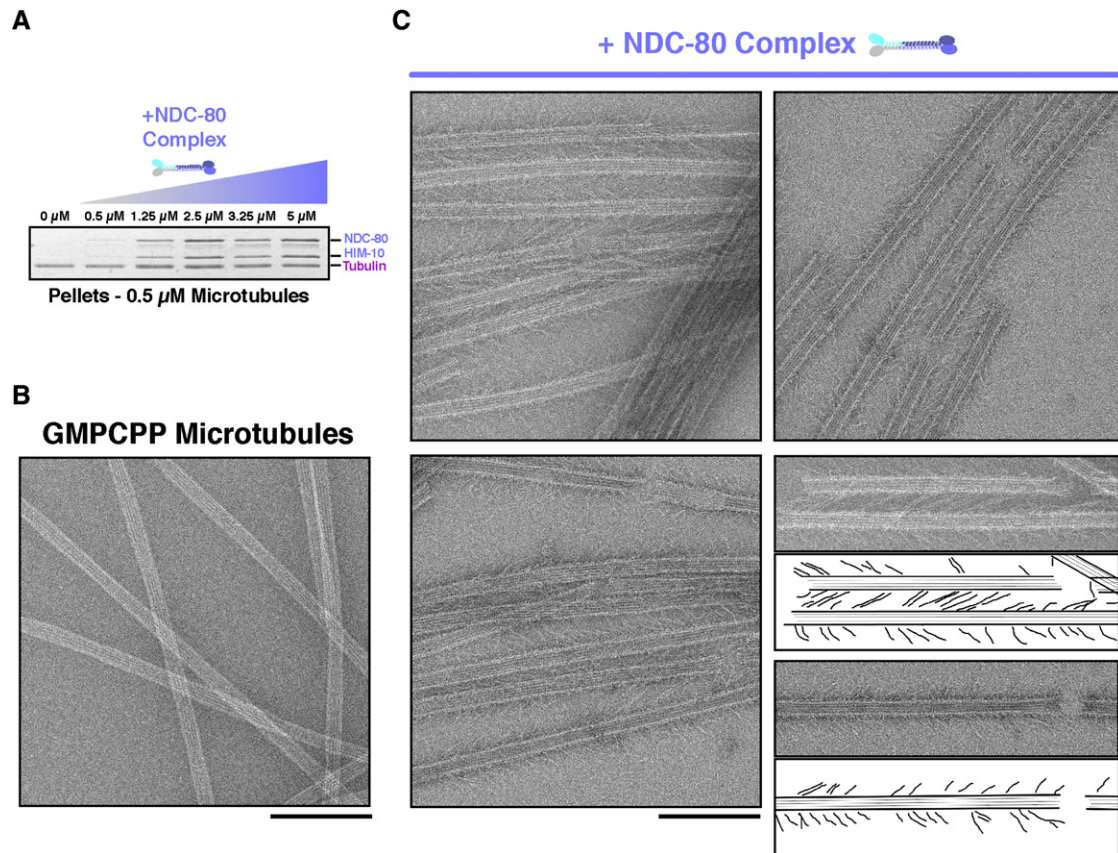
Figure 5. Electron Microscopy of GMPCPP Microtubules with Bound NDC-80 Complexes

(A) Coomassie-stained gel of the pellets from microtubule-binding reactions with 0.5 μM GMPCPP microtubules and increasing amounts of the NDC-80 complex. Densitometry indicates that the saturation stoichiometry is between 1 and 2 NDC-80 complexes per tubulin dimer.

(B) Negatively stained control GMPCPP microtubules.

(C) Negatively stained GMPCPP microtubules in the presence of 5 μM NDC-80 complex. The NDC-80 complex forms angled rod-like projections on the microtubule lattice. Three different representative fields are shown, which include views of interactions between complexes on adjacent microtubules and a microtubule bundle. Traces of the EM images on the bottom right depict the angled rod-like complexes bound to the lattice. Scale bars represent 200 nm.
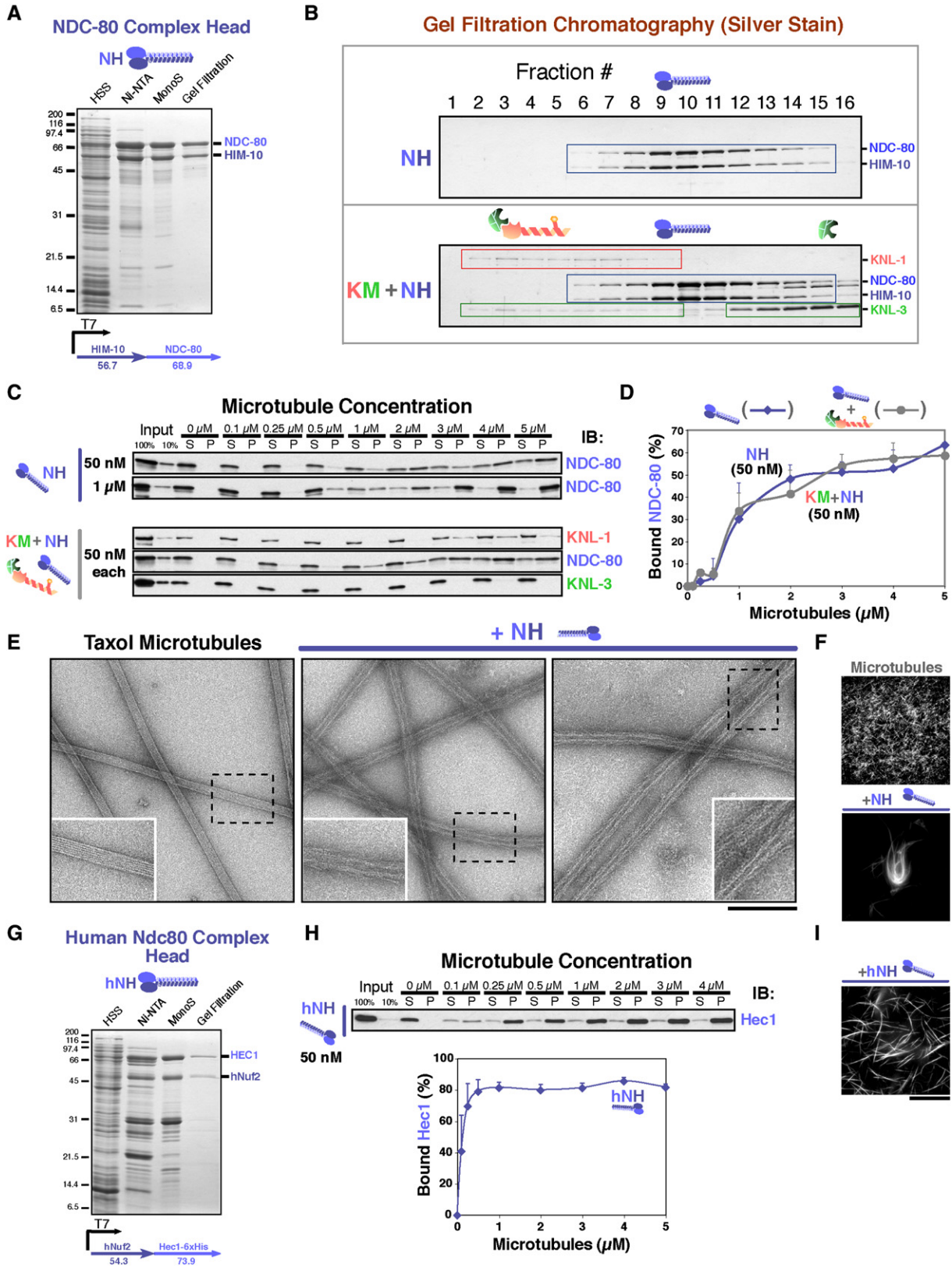
a uniform polarity that resembled the intact complex (Figure 6E). We conclude that the NDC-80/Nuf2^{HIM-10} dimer is responsible for the binding of the NDC-80 complex to microtubules.

To determine whether the NDC-80 complex head also retains the ability to interact with KNL-1/MIS-12 complex, we performed gel filtration experiments (Figure 6B). No shift in the migration of the NDC-80 complex head was observed in the mixture, suggesting that Spc24^{KBP-4} and Spc25^{KBP-3} are required for the interaction of the NDC-80 complex with KNL-1/MIS-12 complex (Figure 6B). Although we were able to coexpress Spc24^{KBP-4} and Spc25^{KBP-3}, they did not form a stable dimer under the conditions used for isolating the intact complex (data not shown), precluding our ability to test whether they are sufficient for the interaction with KNL-1/MIS-12 complex. Consistent with the inability of the NDC-80/Nuf2^{HIM-10} dimer to interact with KNL-1/MIS-12 complex, a mixture of the NDC-80 complex head and KNL-1/MIS-12 complex

did not show a synergistic increase in microtubule-binding activity (Figures 6C and 6D; compare with Figures 4B and 4C). These results demonstrate that a NDC-80/Nuf2^{HIM-10} dimer is sufficient to bind to microtubules and suggest that Spc24^{KBP-4} and Spc25^{KBP-3} are required for the association of the NDC-80 complex with its kinetochore-bound receptor formed by KNL-1 and the MIS-12 complex.

The Human Ndc80 Complex Head Domain Binds to and Bundles Microtubules

The above results indicate that the microtubule-binding activity of the *C. elegans* NDC-80 complex resides in the NDC-80 and Nuf2^{HIM-10} dimer. To test whether microtubule binding by the Ndc80 complex is conserved, we copurified the two homologous subunits of the human Ndc80 complex: Hec1/hNdc80 and hNuf2 (Figure 6G). The human Ndc80 complex head cosedimented with microtubules (Figure 6H) and also bundled them (Figure 6I), similar to the *C. elegans* NDC-80 complex head. We conclude

A NDC-80 Complex Head

NH

NDC-80
HIM-10

200
116
97.4
66
45
31
21.5
14.4
6.5

T7
HIM-10 → NDC-80
56.7   68.9

B Gel Filtration Chromatography (Silver Stain)

Fraction #
1 2 3 4 5 6 7 8 9 10 11 12 13 14 15 16

NH
NDC-80
HIM-10

KM + NH
KNL-1
NDC-80
HIM-10
KNL-3

C Microtubule Concentration

Input 0 µM 0.1 µM 0.25 µM 0.5 µM 1 µM 2 µM 3 µM 4 µM 5 µM IB:
100% 10% S P S P S P S P S P S P S P S P S P

NH 50 nM NDC-80
1 µM NDC-80

KM + NH 50 nM each KNL-1
NDC-80
KNL-3

D

Bound NDC-80 (%)

NH (50 nM)
KM+NH (50 nM)

Microtubules (µM)

E Taxol Microtubules   + NH

F
Microtubules
+NH

G Human Ndc80 Complex Head

hNH

HEC1
hNuf2

200
116
97.4
66
45
31
21.5
14.4
6.5

T7
hNuf2 → Hec1-6xHis
54.3   73.9

H Microtubule Concentration

Input 0 µM 0.1 µM 0.25 µM 0.5 µM 1 µM 2 µM 3 µM 4 µM IB:
100% 10% S P S P S P S P S P S P S P S P

hNH Hec1
50 nM

Bound Hec1 (%)

hNH

Microtubules (µM)

I
+hNH

that the microtubule-binding and -bundling activity of the Ndc80 complex is widely conserved.

Aurora Kinase Phosphorylation of NDC-80 Regulates the Microtubule-Binding Activity of the NDC-80 Complex

In budding yeast, Ndc80 is a target of the Aurora kinase Ipl1 (Cheeseman et al., 2002), whose kinase activity dissociates incorrectly formed kinetochore-microtubule attachments (reviewed in Pinsky and Biggins, 2005). Although the primary sequence of Ndc80 is divergent, an enriched cluster of predicted Aurora kinase phosphorylation sites exists within the N-terminal 100 amino acids of budding yeast, fission yeast, human, and *C. elegans* Ndc80 (Figure 7A, Figure S4). To determine whether the *C. elegans* NDC-80 complex, like the yeast complex, is a direct target of Aurora B, we conducted in vitro phosphorylation reactions. For these experiments, we used Ipl1, the budding yeast Aurora kinase, since it is readily purified in active form and shows a well-conserved phosphorylation pattern (Cheeseman et al., 2002). Ipl1/Aurora B phosphorylated the NDC-80 subunit of the intact NDC-80 complex as well as the head dimer (Figure 7B). No significant phosphorylation of other complex subunits was observed (Figure 7B). Importantly, mutation of the four putative Aurora B phosphorylation sites in the N terminus of NDC-80 (T8, S18, S44, S51; Figure 7A) to alanine virtually eliminated Ipl1-directed phosphorylation (Figure 7B).

In vivo, Aurora B eliminates incorrect kinetochore-microtubule attachments, allowing the reformation of correct bipolar attachments (Tanaka et al., 2002). One possible mechanism for the detachment is that Aurora phosphorylation reduces the affinity of a key microtubule-binding activity at the kinetochore. The NDC-80 complex binds directly to microtubules and is phosphorylated by Aurora B on a subunit that is crucial for its microtubule-binding activity, making it an ideal target for the regulation of kinetochore-microtubule attachments. To investigate this possibility, we assessed microtubule binding after in vitro phosphorylation by Ipl1. A significant reduction in microtubule binding was observed for both the intact complex and the head dimer after incubation with both Ipl1 and ATP, but not with Ipl1 in the absence of ATP (Figures 7C and 7D). ATP addition on its own, without Ipl1, had no effect (not shown). Importantly, the microtubule-binding activity of the phosphorylation site-mutated version of the NDC-80 complex (N^{4A}) was unaffected by treatment with Ipl1 and ATP (Figures 7C and 7D). Thus, phosphorylation of the N terminus of the NDC-80 subunit by Ipl1/Aurora kinase directly modulates the microtubule-binding affinity of the NDC-80 complex.

These results demonstrate that the Ndc80 complex is a conserved Aurora kinase target and suggest that reduction in its microtubule-binding affinity after phosphorylation of the Ndc80 subunit may contribute to Aurora kinase-dependent elimination of incorrect kinetochore-microtubule attachments in vivo.
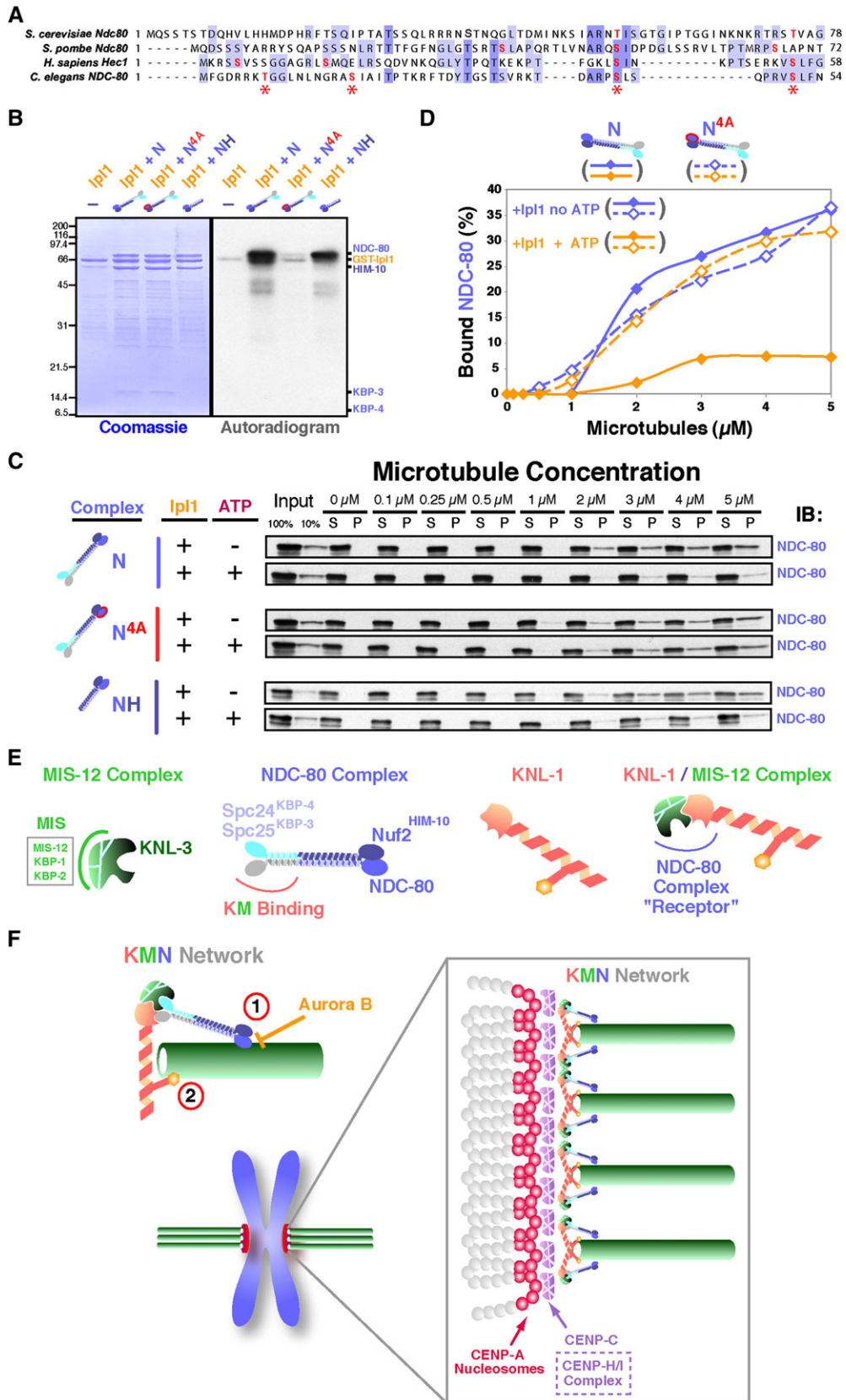
DISCUSSION

A Model for the Core Microtubule-Binding Site of the Kinetochore

Prior in vivo analysis of components of the KNL-1/Mis12 complex/Ndc80 complex (KMN) network in multiple organisms indicated that this network is essential for kinetochore-microtubule interactions. However, it was unclear whether these proteins functioned directly or indirectly to generate microtubule attachments. Based on a combination of the in vitro results presented here and prior in vivo phenotypic analysis (Cheeseman et al., 2004; Desai et al., 2003), we propose that the KMN network constitutes the core microtubule-binding site of the kinetochore (Figures 7E and 7F).

Within the KMN network, the three MIS proteins (MIS-12, KBP-1, and KBP-2) stabilize KNL-3 both in vitro and in vivo (this work; Cheeseman et al., 2004; Kline et al., 2006). On the basis of similarities observed during coexpression, we believe that KNL-3 is equivalent to the Dsn1 subunit of the human Mis12 complex. The Mis12 complex makes an important contribution to kinetochore assembly

Figure 6. The NDC-80 Complex Head Binds to Microtubules, but Does Not Bind to or Synergize with KNL-1/MIS-12 Complex
(A) Purification of the NDC-80 complex head (comprised of NDC-80 and Nuf2^{HIM-10}). Top, Coomassie-stained gel of the purification. Bottom, schematic of the construct used to coexpress NDC-80 and Nuf2^{HIM-10}. Untagged NDC-80 complex head binds to nickel agarose with high affinity.
(B) The NDC-80 complex head does not associate with KNL-1/MIS-12 complex by gel filtration. Silver-stained gels showing the migration of NDC-80 complex head, or NDC-80 complex head mixed with KNL-1/MIS-12 complex as in Figure 2.
(C) The NDC-80 complex head binds directly to microtubules but does not synergize with KNL-1/MIS-12 complex. Cosedimentation analysis of 50 nM or 1 μM NDC-80 complex head alone (monitored by NDC-80 immunoblotting), or 50 nM NDC-80 complex head mixed with 50 nM KNL-1/MIS-12 complex (monitored by immunoblotting KNL-1, KNL-3, and NDC-80) was performed at varying microtubule concentrations as described above.
(D) Graph showing the microtubule-binding activity of 50 nM NDC-80 complex head in the presence or absence of KNL-1/MIS-12 complex (n = 2). Error bars represent standard deviation.
(E) Negative stain electron microscopy showing the decoration of taxol-stabilized microtubules by the NDC-80 complex head. Insets are 1.75×. Scale bar represents 200 nm.
(F) The NDC-80 complex head bundles microtubules. Bundling experiment conducted as in Figure 3C.
(G) Purification of the human Ndc80 complex head (comprised of Hec1/hNdc80 and hNuf2). Top, Coomassie-stained gel of the purification. Bottom, schematic of the construct used to coexpress hNdc80 and Nuf2.
(H) The human Ndc80 complex head binds directly to microtubules. Cosedimentation analysis of 50 nM human Ndc80 complex head (n = 3; monitored by immunoblotting HEC1) was performed at varying microtubule concentrations as described above. Error bars represent standard deviation.
(I) The human Ndc80 complex head bundles microtubules. Scale bar represents 40 μm.

A

```
S. cerevisiae Ndc80  1 MQSSTSTDQHVLHHMDPHRFTSQIPTATSSQLRRRNSTNQGLTDMINKSIARNTISGTGIPTGGINKNKRTRSTVAG 78
   S. pombe Ndc80  1 -----MQDSSSYARRYSQAPSSSNLRTTTFGFNGLGTSRTSLAPQRTLVNARQSIDPDGLSSRVLTPTMRPSLAPNT 72
    H. sapiens Hec1  1 ------MKRSSVSSGGAGRLSMQELRSQDVNKQGLYTPQTKEKPT----FGKLSIN-------KPTSERKVSLFG 58
  C. elegans NDC-80  1 -----MFGDRRKTGGLNLNGRASIAITPTKRFTDYTGSTSVRKT----DARPSLS--------QPRVSLFN 54
                                  *              *                        *              *
```

B

C

Microtubule Concentration

D

E

F

(Cheeseman et al., 2004; Kline et al., 2006; Obuse et al., 2004), and we speculate that the stabilization of KNL-3 by MIS proteins is important for this function. Our in vitro analysis suggests that KNL-1 and the Mis12 complex together generate a binding site for the Ndc80 complex (Figures 7E and 7F). This result, combined with our previous in vivo loss-of-function phenotypic analysis, leads us to propose that the Ndc80 complex receptor at the kinetochore is jointly comprised of KNL-1 and KNL-3 (Figure 7E).

Most importantly, there are two distinct microtubule-binding activities in the KMN network—one that resides in the Ndc80/Nuf2 dimer of the Ndc80 complex and a second in KNL-1 (Figure 7E). Regulation of Ndc80 complex microtubule binding by Aurora B phosphorylation of the Ndc80 subunit is likely to be important in promoting chromosome biorientation by weakening incorrect kinetochore-microtubule interactions. Consistent with this, recent work from DeLuca and coworkers has demonstrated that expression of a Ndc80/Hec1 mutant in human cells which is unable to be phosphorylated by Aurora B, causes an increase in incorrect kinetochore-microtubule attachments and chromosome segregation defects (DeLuca et al., 2006 [this issue of Cell]). The Spc24/Spc25 dimer of the Ndc80 complex is required for association with its kinetochore-bound receptor formed by the KNL-1/Mis12 complex (Figure 7D). This places the Ndc80 complex in the requisite geometry where the microtubule binding Ndc80/Nuf2 half projects out toward the spindle. The intact KMN network is incorporated into the outer kinetochore plate to form the repeating microtubule-binding sites of eukaryotic kinetochores (Figure 7E).

We speculate that the core microtubule-binding site formed by the KMN network is in turn integrated with other microtubule-directed activities localized at kinetochores, such as polymerization-promoting CLASPs, the microtubule-depolymerizing kinesin-13s, and putative Dam1 ring complex orthologs to generate the complex dynamic properties of this interface observed in living cells.

Building a Dynamic Interface with the Spindle: Intrinsic Affinity versus Valency of Interactions at the Kinetochore

A central feature of the kinetochore-spindle interface is its ability to maintain stable associations while bound microtubules are polymerizing or depolymerizing. Such a feature is difficult to reconcile with a high-affinity/low-turnover interaction at core microtubule-binding sites and is better explained by an interaction surface composed of an array of intrinsically low-affinity binding sites. We have demonstrated that two such low-affinity binding sites exist within the KMN network, which synergize in the context of the intact network.

One possibility to explain the synergy in microtubule-binding activity is that the interaction of KNL-1 and the Ndc80 complex within the KMN network enhances either one or both intrinsic affinities via an allosteric mechanism. The Ndc80 complex head dimer consistently shows stronger microtubule-binding activity than the 4-subunit complex (see Figure 3A and Figure 6). One hypothesis to explain this observation is autoinhibition of microtubule-binding activity in the intact Ndc80 complex. Binding to KNL-1/Mis12 complex may relieve this autoinhibition, enhancing the microtubule-binding activity. The synergy in microtubule-binding activity likely also reflects the increased number of physically connected microtubule-binding sites associated with formation of the KMN network. The oligomeric nature of KNL-1 and the need for a dynamic as opposed to static interface with spindle microtubules at the kinetochore both support this idea. Multivalency of low-affinity interactions would also explain how effective microtubule-binding activity is restricted to the kinetochore, where assembly of a dense array of the KMN network is triggered through local interactions with the inner kinetochore. Given their intrinsic low affinities, free Ndc80 complex and KNL-1 would not substantially interact with microtubules at the concentrations present in cytoplasm (estimated to be <50 nM; Emanuele et al., 2005). A proposal that multivalent interactions are important in forming the core microtubule-binding site of the

Figure 7. NDC-80 Complex Microtubule Binding Is Sensitive to Phosphorylation by Aurora B

(A) Alignment of the N-terminal region of Ndc80 homologs from fungi, humans, and *C. elegans* showing identical residues shaded. Sites matching the predicted Aurora B phosphorylation consensus site are indicated in red (see also Figure S4). Asterisks mark the residues in *C. elegans* NDC-80 that were mutated to alanine in the N^{4A} mutant NDC-80 complex.

(B) Ipl1/Aurora B phosphorylates the N terminus of the NDC-80 subunit of the NDC-80 complex in vitro. Coomassie-stained gel of the indicated kinase assay mixtures (left) and the matching autoradiogram (right) are shown.

(C) Microtubule cosedimentation analysis of 50 nM wild-type or mutant NDC-80 complex and NDC-80 complex head (detected by probing for NDC-80) in the presence of Ipl1 alone (no phosphorylation) or Ipl1 plus ATP (phosphorylation).

(D) Graph showing the microtubule-binding activity of the wild-type and N^{4A} mutant NDC-80 complex with Ipl1 in the presence or absence of ATP. The average of two experiments is plotted.

(E) Models for the component parts of the KMN network. The MIS proteins (MIS-12, KBP-1, and KBP-2) directly interact with and stabilize KNL-3. The Spc24/Spc25 dimer of the NDC-80 complex is required to mediate the interaction of the NDC-80 complex with the KNL-1/MIS-12 complex. KNL-1 directly associates with the MIS-12 complex, and this association is necessary to form the kinetochore receptor for the NDC-80 complex.

(F) Microtubule-binding activities of the KMN network. Two distinct microtubule-binding regions are present in the network—one in the NDC-80 complex head and one in KNL-1. NDC-80 complex binding to microtubules is inhibited by Aurora B phosphorylation. Connecting these components within the KMN network synergizes the net microtubule-binding activity. Schematic on the right presents a speculative view of the kinetochore-microtubule interface. The KMN network assembles on a specialized chromatin domain formed by CENP-A nucleosomes, CENP-C, and other inner kinetochore proteins to form a repeating unit allowing interactions with multiple microtubules.

kinetochore is also consistent with recent measurements indicating the presence of 5–8 individual KNL-1/Spc105 molecules, Mis12 complexes, and Ndc80 complexes at the single-microtubule-binding site of the budding yeast kinetochore (Joglekar et al., 2006).

EXPERIMENTAL PROCEDURES

Protein Purification

C. elegans open reading frames were amplified from N2 cDNA and cloned into the polycistronic transfer vector pET3aTr, and then into the polycistronic expression construct pST39 (Tan, 2001); tags were added as indicated in Figure 1. For coexpression of KNL-1-6xHis and the MIS-12 complex, the MIS-12 polycistron was cloned into pColaDuet-1 (Novagen). Phosphorylation sites were mutated with Quikchange (Stratagene).

Protein expression in BL21 (DE3) *E. coli* was induced with 0.1 mM IPTG for 3–4 hr at 20°C. Cells were lysed in Lysis Buffer (50 mM Na Phosphate [pH 8.0], 300 mM NaCl, 10 mM imidazole, 0.1% Tween-20, 5 mM β-mercaptoethanol [BME]) and clarified at 42,000 × g for 30 min at 4°C. In some cases (Figure 1), clarified extract was fractionated by 20% ammonium sulfate precipitation and the pellet resuspended in Lysis buffer with 100 mM NaCl. Ni-NTA agarose (Qiagen) was incubated with clarified lysates or resuspended ammonium sulfate pellets for 45 min, washed with Wash Buffer (50 mM Na Phosphate [pH 8.0], 400 mM NaCl, 10 mM imidazole, 0.1% Tween-20, 5 mM BME), and eluted with 50 mM Na Phosphate (pH 7.0), 400 mM NaCl, 250 mM imidazole, 5 mM BME. The eluted protein was exchanged into S buffer (50 mM Na Phosphate [pH 7.0], 50 mM NaCl, 1 mM EDTA, 1 mM BME) with a EconoPac PD10 desalting column (BioRad). For cation exchange, the protein was bound to SP sepharose (GE Biosciences) and eluted with S buffer with 500 mM NaCl followed by desalting to reduce the salt concentration to 50 mM NaCl, or exchange protein into BRB80 (80 mM PIPES [pH 6.8], 1 mM EGTA, 1 mM MgCl$_2$). Gel filtration was conducted in S buffer on a Superose 6 column. Protein concentrations were determined with a combination of Bradford protein assays and densitometry of Coomassie-stained gels relative to a BSA standard. For the MIS-12 complex and the KNL-1/MIS-12 complex, the reported concentrations are for the KNL-3 subunit.

Microtubule Cosedimentation Assays

Microtubule assembly and measurement of polymeric tubulin concentration were performed as described (Desai et al., 1999). For microtubule-binding reactions, MonoS or gel filtration purified proteins were diluted in S buffer, 0.5 mg/ml BSA was added, and the mix was precleared at 90,000 rpm for 10 min in a TLA100 rotor. 10 μl of the supernatant was mixed with 10 μl of microtubules diluted in BRB80 to result in a final microtubule concentration indicated in each figure. Reactions were incubated at room temperature for 10 min, pipetted onto 120 μl of BRB80 + 40% glycerol and pelleted for 10 min at 80,000 rpm in a TLA100 rotor at 25°C. For the supernatant sample, 40 μl was removed from the top of the tube. For the pellet sample, the remaining supernatant was removed and 40 μl BRB80 + 10 mM CaCl$_2$ was added to the pellet for 10 min on ice. Equivalent amounts of supernatant (S) and pellet (P) fractions were immunoblotted and exposures were chosen to maximize dynamic range. In cases where the concentration of input complexes was varied, the final sample was diluted to load equivalent amounts to a 50 nM input. In vitro phosphorylation and kinase assays were conducted as described (Cheeseman et al., 2002) with proteins in BRB80 buffer. For the microtubule-binding experiments, a 50 μl kinase reaction was diluted with 100 μl BRB80 + 1 mg/ml BSA.

Electron Microscopy

Mixtures of the NDC-80 complex and GMPCPP microtubules were applied to glow-discharged, carbon-coated grids, negatively stained with 1% uranyl acetate, and imaged with a Phillips Technai F20 transmission electron microscope operating at 120 kV. Images were collected at 1.5–2.0 μm underfocus with a 4 K by 4 K Gatan CCD camera at a nominal magnification of 50,000×, corresponding to 2.24 Å per pixel. For the NDC-80 complex head, 0.25 mg/ml taxol-stabilized microtubules were first applied to grids and then incubated for 1–2 min with 4 μM head dimer. Images were acquired with a Phillips CM120 transmission electron microscope operating at 120 kV with a 2 K by 2 K Gatan CCD camera at a nominal magnification of 22,000×.

Supplemental Data

Four Supplemental Figures can be found with this article online at http://www.cell.com/cgi/content/full/127/5/983/DC1/.

REFERENCES

Cheeseman, I.M., Brew, C., Wolyniak, M., Desai, A., Anderson, S., Muster, N., Yates, J.R., Huffaker, T.C., Drubin, D.G., and Barnes, G. (2001). Implication of a novel multiprotein Dam1p complex in outer kinetochore function. J. Cell Biol. *155*, 1137–1146.

Cheeseman, I.M., Anderson, S., Jwa, M., Green, E.M., Kang, J., Yates, J.R., III, Chan, C.S., Drubin, D.G., and Barnes, G. (2002). Phospho-regulation of kinetochore-microtubule attachments by the Aurora kinase Ipl1p. Cell *111*, 163–172.

Cheeseman, I.M., Niessen, S., Anderson, S., Hyndman, F., Yates, J.R., III, Oegema, K., and Desai, A. (2004). A conserved protein network controls assembly of the outer kinetochore and its ability to sustain tension. Genes Dev. *18*, 2255–2268.

Ciferri, C., De Luca, J., Monzani, S., Ferrari, K.J., Ristic, D., Wyman, C., Stark, H., Kilmartin, J., Salmon, E.D., and Musacchio, A. (2005). Architecture of the human ndc80-hec1 complex, a critical constituent of the outer kinetochore. J. Biol. Chem. *280*, 29088–29095.

Cleveland, D.W., Mao, Y., and Sullivan, K.F. (2003). Centromeres and kinetochores: from epigenetics to mitotic checkpoint signaling. Cell *112*, 407–421.

De Wulf, P., McAinsh, A.D., and Sorger, P.K. (2003). Hierarchical assembly of the budding yeast kinetochore from multiple subcomplexes. Genes Dev. *17*, 2902–2921.

DeLuca, J.G., Dong, Y., Hergert, P., Strauss, J., Hickey, J.M., Salmon, E.D., and McEwen, B.F. (2005). Hec1 and nuf2 are core components of the kinetochore outer plate essential for organizing microtubule attachment sites. Mol. Biol. Cell *16*, 519–531.

DeLuca, J.G., Gall, W.E., Ciferri, C., Cimini, D., Musacchio, A., and Salmon, E.D. (2006). Kinetochore microtubule dynamics and attachment stability are regulated by Hecl. Cell *127*, this issue, 969–982.

Desai, A., Verma, S., Mitchison, T.J., and Walczak, C.E. (1999). Kin I kinesins are microtubule-destabilizing enzymes. Cell *96*, 69–78.

Desai, A., Rybina, S., Muller-Reichert, T., Shevchenko, A., Shevchenko, A., Hyman, A., and Oegema, K. (2003). KNL-1 directs assembly of the microtubule-binding interface of the kinetochore in *C. elegans*. Genes Dev. *17*, 2421–2435.

Emanuele, M.J., McCleland, M.L., Satinover, D.L., and Stukenberg, P.T. (2005). Measuring the stoichiometry and physical interactions between components elucidates the architecture of the vertebrate kinetochore. Mol. Biol. Cell *16*, 4882–4892.

Howell, B.J., McEwen, B.F., Canman, J.C., Hoffman, D.B., Farrar, E.M., Rieder, C.L., and Salmon, E.D. (2001). Cytoplasmic dynein/dynactin drives kinetochore protein transport to the spindle poles and has a role in mitotic spindle checkpoint inactivation. J. Cell Biol. *155*, 1159–1172.

Joglekar, A.P., Bouck, D.C., Molk, J.N., Bloom, K.S., and Salmon, E.D. (2006). Molecular architecture of a kinetochore-microtubule attachment site. Nat. Cell Biol. *8*, 581–585.

Kar, S., Fan, J., Smith, M.J., Goedert, M., and Amos, L.A. (2003). Repeat motifs of tau bind to the insides of microtubules in the absence of taxol. EMBO J. *22*, 70–77.

Kline, S.L., Cheeseman, I.M., Hori, T., Fukagawa, T., and Desai, A. (2006). The human Mis12 complex is required for kinetochore assembly and proper chromosome segregation. J. Cell Biol. *173*, 9–17.

Kline-Smith, S.L., Sandall, S., and Desai, A. (2005). Kinetochore-spindle microtubule interactions during mitosis. Curr. Opin. Cell Biol. *17*, 35–46.

Maddox, P., Straight, A., Coughlin, P., Mitchison, T.J., and Salmon, E.D. (2003). Direct observation of microtubule dynamics at kinetochores in *Xenopus* extract spindles: implications for spindle mechanics. J. Cell Biol. *162*, 377–382.

Maiato, H., DeLuca, J., Salmon, E.D., and Earnshaw, W.C. (2004). The dynamic kinetochore-microtubule interface. J. Cell Sci. *117*, 5461–5477.

Maiato, H., Khodjakov, A., and Rieder, C.L. (2005). *Drosophila* CLASP is required for the incorporation of microtubule subunits into fluxing kinetochore fibres. Nat. Cell Biol. *7*, 42–47.

McCleland, M.L., Kallio, M.J., Barrett-Wilt, G.A., Kestner, C.A., Shabanowitz, J., Hunt, D.F., Gorbsky, G.J., and Stukenberg, P.T. (2004). The vertebrate Ndc80 complex contains Spc24 and Spc25 homologs, which are required to establish and maintain kinetochore-microtubule attachment. Curr. Biol. *14*, 131–137.

Nekrasov, V.S., Smith, M.A., Peak-Chew, S., and Kilmartin, J.V. (2003). Interactions between centromere complexes in *Saccharomyces cerevisiae*. Mol. Biol. Cell *14*, 4931–4946.

Obuse, C., Iwasaki, O., Kiyomitsu, T., Goshima, G., Toyoda, Y., and Yanagida, M. (2004). A conserved Mis12 centromere complex is linked to heterochromatic HP1 and outer kinetochore protein Zwint-1. Nat. Cell Biol. *6*, 1135–1141.

Pinsky, B.A., and Biggins, S. (2005). The spindle checkpoint: tension versus attachment. Trends Cell Biol. *15*, 486–493.

Putkey, F.R., Cramer, T., Morphew, M.K., Silk, A.D., Johnson, R.S., McIntosh, J.R., and Cleveland, D.W. (2002). Unstable kinetochore-microtubule capture and chromosomal instability following deletion of CENP-E. Dev. Cell *3*, 351–365.

Rieder, C.L. (1982). The formation, structure, and composition of the mammalian kinetochore and kinetochore fiber. Int. Rev. Cytol. *79*, 1–58.

Rieder, C.L., and Salmon, E.D. (1998). The vertebrate cell kinetochore and its roles during mitosis. Trends Cell Biol. *8*, 310–318.

Sanchez-Perez, I., Renwick, S.J., Crawley, K., Karig, I., Buck, V., Meadows, J.C., Franco-Sanchez, A., Fleig, U., Toda, T., and Millar, J.B. (2005). The DASH complex and Klp5/Klp6 kinesin coordinate bipolar chromosome attachment in fission yeast. EMBO J. *24*, 2931–2943.

Schrader, F. (1953). Mitosis: The Movement of Chromosomes in Cell Division, Second Edition (New York: Columbia University Press).

Tan, S. (2001). A modular polycistronic expression system for overexpressing protein complexes in Escherichia coli. Protein Expr. Purif. *21*, 224–234.

Tanaka, T.U., Rachidi, N., Janke, C., Pereira, G., Galova, M., Schiebel, E., Stark, M.J.R., and Nasmyth, K. (2002). Evidence that the Ipl1-Sli15 (Aurora Kinase-INCENP) complex promotes chromosome bi-orientation by altering kinetochore-spindle pole connections. Cell *108*, 317–329.

Wei, R.R., Sorger, P.K., and Harrison, S.C. (2005). Molecular organization of the Ndc80 complex, an essential kinetochore component. Proc. Natl. Acad. Sci. USA *102*, 5363–5367.

Wigge, P.A., and Kilmartin, J.V. (2001). The Ndc80p complex from *Saccharomyces cerevisiae* contains conserved centromere components and has a function in chromosome segregation. J. Cell Biol. *152*, 349–360.